Return-Loss Investigation of the Equivalent Width of Substrate-Integrated Waveguide Circuits

Farzaneh Taringou and Jens Bornemann

Department of Electrical and Computer Engineering, University of Victoria, Victoria, BC, V8W 3P6, Canada

***Abstract* — Five different models to determine the equivalent width of substrate-integrated waveguide (SIW) circuits are investigated. The reflection coefficients between all-dielectric waveguides of equivalent width and SIW circuits are analyzed by full-wave techniques. It is found that one of the models yields consistently inferior results while the others depend on the ratio of the via-hole diameter and the center-to-center spacing of the via holes. Moreover, the influence of the substrate's permittivity with respect to the via-hole diameter and spacing is demonstrated. Recommendations are derived as to the use of respective models for different via diameters and spacings.**

***Index Terms* — Substrate-integrated waveguides, transitions, waveguides, waveguide modes.**

I. Introduction

Substrate-integrated circuits have become an attractive option for millimeter-wave applications as they present a reasonable compromise between planar integrated circuits and all-metal waveguide technology [1]. Especially the substrate-integrated waveguide [SIW] has been extensively used to replace regular waveguide components up to the W-band, e.g. [2].

In order to make use of the large variety of waveguide design guidelines for the design of SIW circuits, the equivalent waveguide width of a SIW is of fundamental importance. It is also imperative in modeling SIW ports in commercially available software packages such as CST and HFSS. Therefore, a number of procedures to determine the SIW's equivalent waveguide width "a_{equ}" have been proposed in the literature, e.g., [3] – [8]. These models take into account (c.f. Fig. 1a) the via hole diameter "d", the longitudinal center-to-center spacing "p", and the transverse center-to-center spacing "a". However, they fail to address the fact that the transition between an equivalent all-dielectric waveguide and the SIW structure should provide minimum reflections over a wide frequency range. Moreover, the permittivity of the dielectric substrate is not included in the models since a transition to an equivalent waveguide is not considered.

Therefore, this paper compares five different approaches to calculate the equivalent waveguide width of SIW circuits. The SIW parameters are chosen according to a range of practical applications in which the equivalent waveguide width is used at some stages in the design process, e.g. [3] – [6], [8] – [12]. It will be shown that the different models produce higher or lower reflection, depending on the ratio d/p of via diameter to spacing. Moreover, the influence of the substrate's permittivity is demonstrated.

II. Equivalent Waveguide Models

Fig. 1a shows 20 circular via-hole pairs connected to all-dielectric waveguides of equivalent width "a_{equ}". Given the via hole diameter "d", the longitudinal center-to-center spacing "p", and the transverse center-to-center spacing "a", the following models from the literature are used to compute the equivalent waveguide width. Note that the respective nomenclature has been adapted to the one used here and that the models will later be referred to by their equation numbers in this paper.

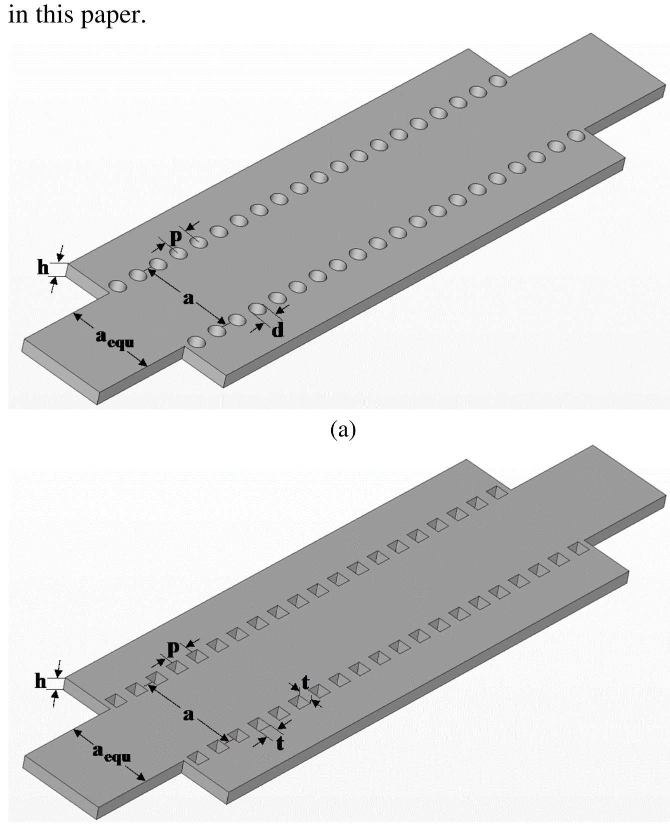

Fig. 1. Substrate-integrated waveguide formed by 20 pairs of via holes and connected to an all-dielectric waveguide of equivalent width; (a) circular via holes, (b) square via holes.

A very simple model is given in [3] as

$$a_{equ} = a - \frac{d^2}{0.95p} \quad (1)$$

A more involved expression is presented in [4]

$$a_{equ} = a\left[x_1 + \frac{x_2}{\frac{p}{d} + \frac{x_1 + x_2 - x_3}{x_3 - x_1}} \right] \quad (2)$$

where $x_1 = 1.0198 + \frac{0.3465}{a/p - 1.0684}$, $x_2 = -0.1183 - \frac{1.2729}{a/p - 1.2010}$

and $x_3 = 1.0082 - \frac{0.9163}{a/p - 0.2152}$.

The expression presented in [5] is a modification of [1] to include the SIW width "a".

$$a_{equ} = a - 1.08\frac{d^2}{p} + 0.1\frac{d^2}{a} \quad (3)$$

A transcendental equation is posted in [6] that must be solved numerically for "a_{equ}".

$$a = \frac{2a_{equ}}{\pi} \operatorname{arcctg}\left[\frac{\pi p}{4a_{equ}} \ln \frac{p}{2d} \right] \quad (4)$$

Finally, a more recently published formula in [7] is

$$a_{equ} = \frac{a}{\sqrt{1 + \left(\frac{2a-d}{p}\right)\left(\frac{d}{a-d}\right)^2 - \frac{4a}{5p^4}\left(\frac{d^2}{a-d}\right)^3}} \quad (5)$$

and [7] also discusses methods (1), (3) and (4) above.

Recently, new fabrication techniques have permitted the designing engineer to use via holes of different cross sections, e.g. [2], which has led to applications involving square via holes [13], [14] and a respective modeling technique based on the mode-matching technique (MMT) [15]. Referring to Fig. 1b, the square via-hole dimensions are straightforwardly obtained from the circular ones by letting them occupy the same cross section.

$$t = 0.5d\sqrt{\pi} \quad (6)$$

In order to place a SIW circuit within a certain frequency range, the equivalent waveguide width is related to the cutoff frequency by

$$a_{equ} = \frac{c}{2f_c\sqrt{\varepsilon_r}} \quad (7)$$

where "c" is the speed of light and ε_r the permittivity of the substrate. For a given d/p ratio, the cutoff frequency of 15 GHz used in this paper is obtained from (7) by iteratively solving (2) for the transverse center-to-center spacing "a" (c.f. Fig. 1a). Since the structures in Fig. 1 are symmetric, the next higher-order mode to be excited in the SIW is the TE_{30} mode with a cutoff frequency of 45 GHz.

Among the large number of papers presenting practical examples of SIW technology, the d/p ratio changes from 0.37 [8] to 0.83 [12] with many others somewhere in between these limits. Therefore, this paper investigates ratios of d/p=0.4, 0.6 and 0.8 with the spacing being fixed as p=1.2mm. As far as substrates are concerned, we opted for RT6002 (ε_r=2.94, h=762µm), RT 6006 (ε_r=6.15, h=625µm) and RT6010 (ε_r=10.2, h=254µm).

III. Results

Except for the cutoff frequency of the equivalent waveguide, the permittivity of the substrate is absent from the five models presented in Section II. Therefore, we address this issue first.

Fig. 2 shows the performance of the structure in Fig. 1b and its dependence of the substrate. The initial design with d/p=0.7 and conversion according to (6) was done for ε_r=2.94 and is shown as the red solid line. In selecting a higher dielectric constant, the waveguide width "a" is adjusted (reduced) to maintain the same cutoff frequency. However, the via dimension t and spacing p is maintained since neither of the models (1) - (5) include provisions of ε_r. This results in return loss performances which are worse than the initial design as shown as dotted (blue) and dashed (green) lines in Fig. 2 for permittivities of 6.15 and 10.2, respectively. Only if the via dimensions and spacing are scaled by the square root of ratios of the two substrate materials $\sqrt{2.94/10.2}$, then the initial design is reproduced as shown by the dash-dotted (black) line for ε_r=10.2 in Fig. 2 which coincides with the solid (red) line for ε_r=2.94.

Of course, in scaling a design, via diameters and spacing have to be considered. However, the results presented here indicate that for a given substrate, the choice of via diameter and spacing should be adjusted to provide the best return loss for the transition to the equivalent waveguide. Only then can components with low return-loss requirements be designed effectively.

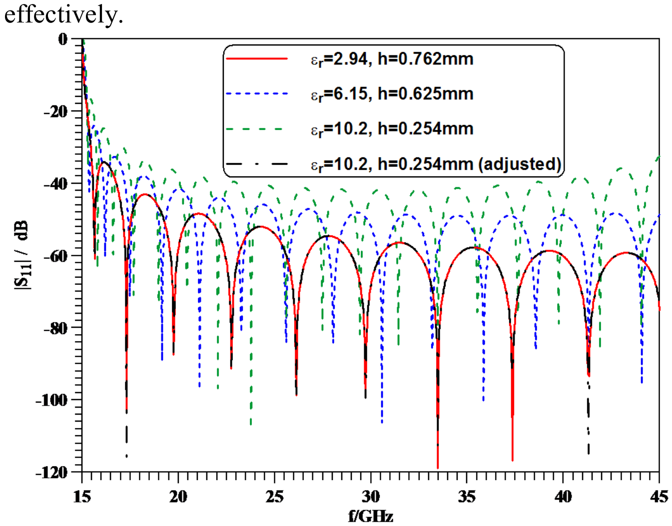

Fig. 2. Return-loss performance of the structure in Fig. 1b with square via holes and its dependence on the permittivity of the substrate (d/p=0.7).

Based on these results, the investigation of the different models for the equivalent waveguide width is conducted only for ε_r=6.15 with h=625µm. Fig. 3 shows a return loss comparison of models (1) – (5) computed by HFSS using circular vias (Fig. 1a) and the MMT with square vias (Fig. 1b), both for d/p=0.4.

At return loss levels between 30 and 40 dB, it can hardly be expected that the results are identical. What is more important, though, is the fact that the trend is the same. Both full-wave codes show that the return loss obtained with models (1), (2), (3) and (5) are almost identical and that model (4) yields inferior results. Thus the equivalent waveguide width computed by model (4) is less accurate than that of the other four since its return loss is worse over the entire frequency range.

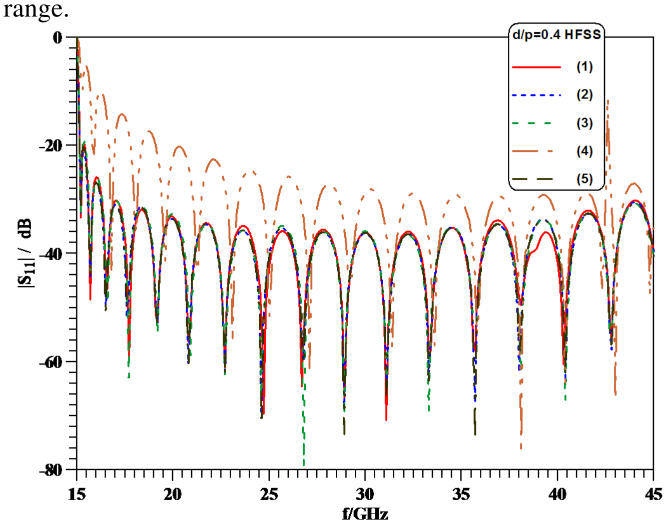

(a)

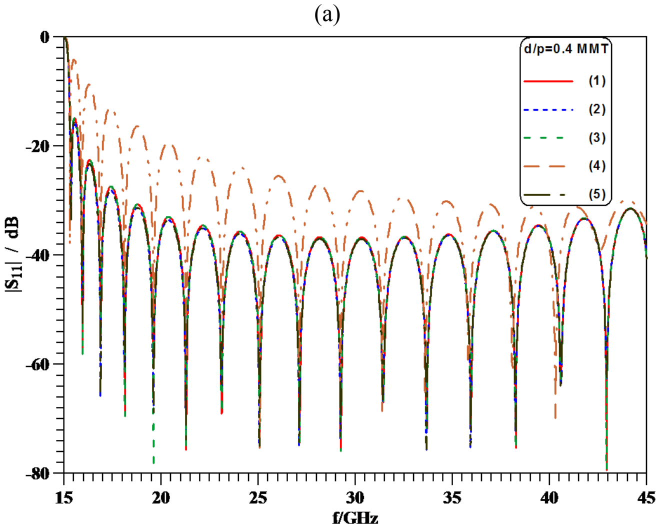

(b)

Fig. 3. Return-loss performances of the equivalent waveguide models (1) – (5) for d/p=0.4; (a) circular via holes (Fig. 1a) calculated with HFSS, (b) square via holes (Fig. 1b) calculated with MMT.

As the via hole diameter increases to d/p=0.6, this trend changes as predicted by HFSS for circular vias (Fig. 4a) and the MMT for square vias (Fig. 4b). For this ratio of via-hole diameter to spacing, model (2) appears to be slightly better than models (1), (3) and (5), which yield almost identical results. The results obtained for model (4) are also inferior for this d/p ratio.

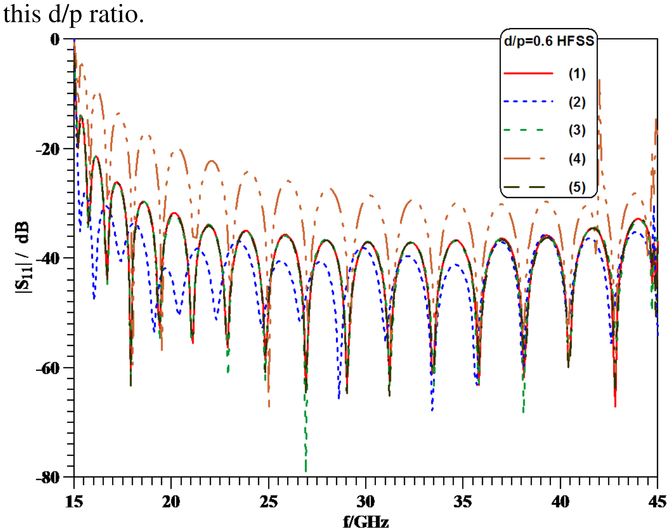

(a)

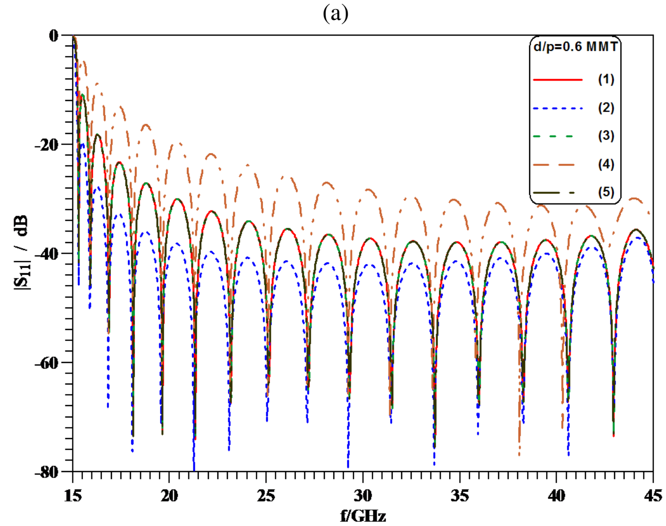

(b)

Fig. 4. Return-loss performances of the equivalent waveguide models (1) – (5) for d/p=0.6; (a) circular via holes (Fig. 1a) calculated with HFSS, (b) square via holes (Fig. 1b) calculated with MMT.

As shown in Fig. 5, the trend changes again for d/p=0.8. Here models (1) and (3) are outperforming models (2) and (5), and all of them are significantly better that model (4). Note that the peak for model (4) in Fig. 5a, and similar ones in Fig. 3a and Fig. 4a, are due to the fact that model (4) consistently predicts wider equivalent waveguide width than the other models. Thus the cutoff frequency falls below 15 GHz and the next excited higher-order mode appears below 45 GHz.

IV. CONCLUSIONS

The investigation of five different models to determine the equivalent waveguide width of SIW circuits concludes with the following recommendations:

First, the substrate's permittivity influences the return loss between the SIW and the equivalent waveguide and thus the via hole diameter and spacing of via holes need to be adjusted in low return-loss designs. Secondly, one of the models yields consistently inferior results than the other four. Thirdly, the remaining four models are by and large equivalent, but best results are obtained when their dependence on the ratio of the via diameter and the center-to-center spacing of the via holes is taken into account.

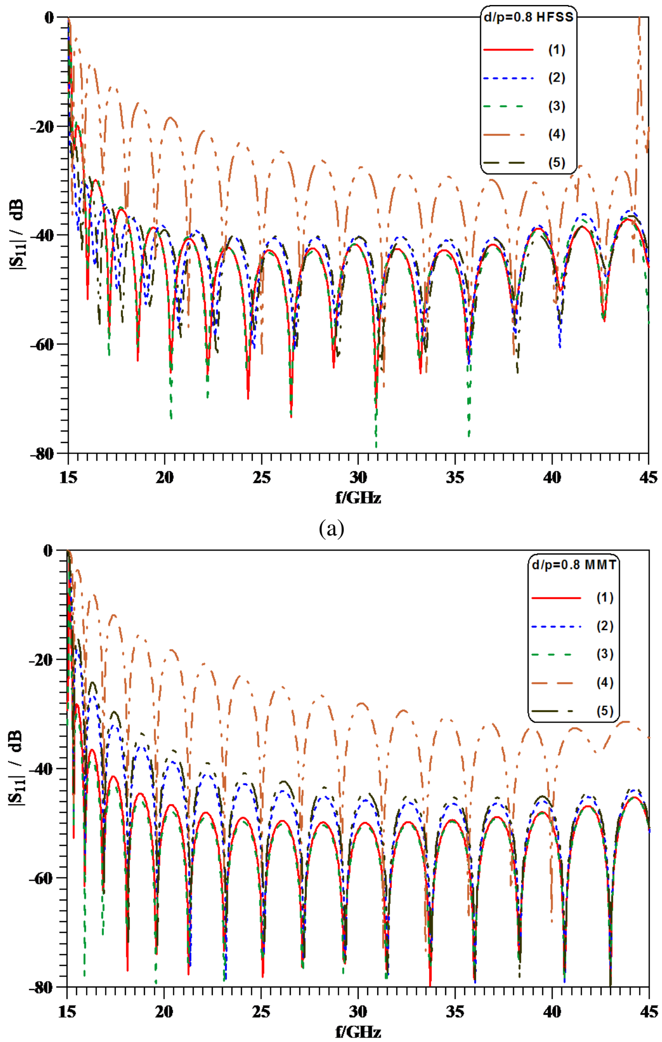

(a)

(b)

Fig. 4. Return-loss performances of the equivalent waveguide models (1) – (5) for d/p=0.8; (a) circular via holes (Fig. 1a) calculated with HFSS, (b) square via holes (Fig. 1b) calculated with MMT.

ACKNOWLEDGEMENT

The authors wish to acknowledge support for this work from the Natural Sciences and Engineering Research Council of Canada and the TELUS Research Grant in Wireless Communications.

REFERENCES

[1] K. Wu, "State-of-the-art and future perspective of substrate integrated circuits (SICs)," *Workshop Notes: Substrate Integrated Circuits (SICs)*, IEEE MTT-S Int. Microwave Symp., Anaheim, USA, May 2010.

[2] E. Moldovan, R.G. Bosisio, and K. Wu, "W-band multiport substrate-integrated waveguide circuits," *IEEE Trans. Microwave Theory Tech.*, vol. 54, pp. 625-632, Feb. 2006.

[3] Y. Cassivi, L. Perregrini, P. Arcioni, M. Bressan, K. Wu, and G. Conciauro, "Dispersion characteristics of substrate integrated rectangular waveguide," *IEEE Microwave Wireless Comp. Lett.*, vol 12, pp. 333-335, Sep. 2002.

[4] L. Yan, W. Hong, G. Hua, J. Chen, K. Wu, and T.J. Cui, "Simulation and experiment on SIW slot array antennas," *IEEE Microwave Wireless Comp. Lett.*, vol. 14, pp. 446-448, Sep. 2004.

[5] F. Xu and K. Wu, "Guided-wave and leakage characteristics of substrate integrated waveguide," *IEEE Trans. Microwave Theory Tech.*, vol. 54, pp. 66-73, Jan. 2005.

[6] W. Che, K. Deng, D. Wang and Y.L. Chow, "Analytical equivalence between substrate-integrated waveguide and rectangular waveguide," *IET Microw. Antennas Propag.*, vol. 2, pp. 35–41, Feb. 2008.

[7] M. Salehi and E. Mehrshahi, "A closed-form formula for dispersion characteristics of fundamental SIW Mode," *IEEE Microwave Wireless Comp. Lett.*, vol 21, pp. 4-6, Jan. 2011.

[8] L.-S. Wu, X.-L. Zhou and W.-Y. Yin, "A novel multilayer partial H-plane filter implemented with folded substrate integrated waveguide (FSIW)," *IEEE Microwave Wireless Comp. Lett.*, vol. 19, pp. 494-496, Aug. 2009.

[9] E. Mehrshahi, M. Salehi, and R. Rezaiesarlak, "Substrate integrated waveguide filters with stopband performance improvement," *Proc. ICMMT*, pp. 2018-2020, Chengdu, China, May 2010.

[10] Y. Cassivi, D. Deslandes and K. Wu, "Substrate integrated waveguide directional couplers," *Proc. Asia-Pacific Microwave Conf.*, FR1B-3, 4 p., Kyoto, Japan, Nov. 2002.

[11] Y.D. Dong, T. Yang and T. Itoh, "Substrate integrated waveguide loaded by complementary split-ring resonators and its applications to miniaturized waveguide filters," *IEEE Trans. Microwave Theory Tech.*, vol. 57, pp. 2211-2223, Sep. 2009.

[12] Q. Lai, C. Fumeaux, W. Hong and R. Vahldieck, "Characterization of the propagation properties of the half-mode substrate integrated waveguide," *IEEE Trans. Microwave Theory Tech.*, vol. 57, pp. 1996-2004, Aug. 2009.

[13] I. Wood, D. Dousset, J. Bornemann and S. Claude, "Linear tapered slot antenna with substrate integrated waveguide feed," *2007 IEEE AP-S Int. Symp. Dig.*, pp. 4761-4764, Honolulu, USA, June 2007.

[14] D. Dousset, K. Wu and S. Claude, "Millimetre-wave broadband transition of substrate-integrated waveguide to rectangular waveguide," *Electron. Lett.*, vol 46, pp. 1610–1611, Nov. 2010.

[15] J. Bornemann and F. Taringou, "Mode-matching analysis of substrate-integrated waveguide circuits", *Proc. Canadian Conf. Elec. Comp. Engr.*, pp. 579-582, Niagara Falls, Canada, May 2011.